

Three dimensional silicon photonic crystals fabricated by two photon phase mask lithography

D. Shir,¹ E. C. Nelson,¹ Y. C. Chen,¹ A. Brzezinski,¹ H. Liao,¹ P. V. Braun,^{1,2} P. Wiltzius,^{1,2} K. H. A. Bogart,³ and J. A. Rogers^{1,2,a)}

¹Department of Materials Science and Engineering, University of Illinois at Urbana-Champaign, Urbana, Illinois 61801, USA

²Beckman Institute for Advanced Science and Technology, University of Illinois at Urbana-Champaign, Urbana, Illinois 61801, USA

³Sandia National Laboratories, Albuquerque, New Mexico 87123, USA

(Received 26 August 2008; accepted 5 November 2008; published online 5 January 2009)

We describe the fabrication of silicon three dimensional photonic crystals using polymer templates defined by a single step, two-photon exposure through a layer of photopolymer with relief molded on its surface. The resulting crystals exhibit high structural quality over large areas, displaying geometries consistent with calculation. Spectroscopic measurements of transmission and reflection through the silicon and polymer structures reveal excellent optical properties, approaching properties predicted by simulations that assume ideal layouts. © 2009 American Institute of Physics. [DOI: 10.1063/1.3036955]

Three dimensional (3D) photonic crystals are of interest for their potential to enable technologies such as low threshold lasers through control of spontaneous emission¹ and compact routing via low-loss optical waveguides in three dimensions.² From a practical standpoint, the main challenge in achieving these types of devices lies in the fabrication of the required precise, submicron 3D crystal structures. Many fabrication methods show promise, including colloidal self-assembly,³ two-photon (2ph) or ink direct writing,^{4,5} and multibeam interference lithography.⁶⁻⁸ Of these methods, interference lithography is attractive for its ability to pattern large areas at high speeds. The main disadvantages are the experimental complexities and the limited practical levels of engineering control over the structure geometries. Recent work with phase mask optics,⁹⁻¹² particularly with those that use conformable elements or molded relief to enable intimate contact mode exposures,⁹⁻¹¹ avoid some of these challenges. We refer to these methods as proximity field nanopatterning techniques (PnP). This paper demonstrates the ability of PnP in a maskless, 2ph mode¹³ to form templates for silicon/air photonic crystals with excellent optical properties, thereby establishing it as a competitive alternative and/or complement to other more widely explored techniques.

Maskless PnP uses molded patterns of relief in a photopolymer as the phase modulating element.^{10,14} Schematic illustrations of the molding process are provided in Figs. 1(a) and 1(b). The mold is made of a slab of the elastomer poly-(dimethylsiloxane) (Dow Corning) elastomer with surface relief in the form of a square array of holes with hole diameter (d), periodicity (p), and relief depth (rd) of $d=400$ nm, $p=540$ nm, and $rd=400$ nm, respectively. Pictures of the mold and the molded photopolymer layer are shown in Figs. 1(c) and 1(d), respectively. Scanning electron micrographs (SEMs) of the relief in the photopolymer are presented in Figs. 1(e) and 1(f).

The molded photopolymer layer served as both the optical phase mask and the recording media for 3D patterning. Blanket exposures of this material followed by removal of

the unexposed regions in a development process produced high quality 3D structures over large areas, via 2ph effects. This procedure enables (i) efficient optical coupling of the exposure light into the photopolymer due to the use of molded relief instead of a separate phase mask, (ii) high contrast exposure due to the quadratic intensity dependence of 2ph absorption, and (iii) simple experimental setup. In this work, an amplified Ti:sapphire laser (Spectra-Physics, Spitfire Pro) with wavelength of 800 nm, repetition rate of 1 kHz, average power of ~ 2 W, and pulse width of ~ 140 fs

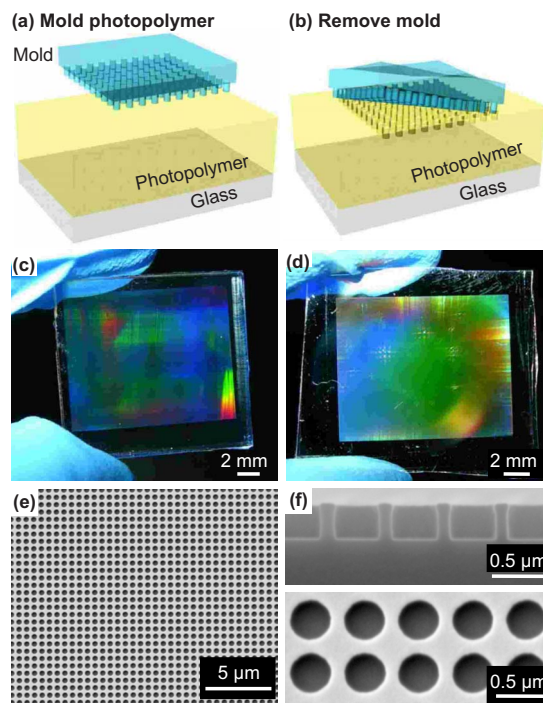


FIG. 1. (Color online) Schematic illustrations, optical, and SEM images of the process for fabricating embossed relief on a layer of a photopolymer for subsequent use in an optical method to form 3D structures in the polymer. [(a) and (b)] Schematic illustrations of the molding step. [(c) and (d)] Optical image of the phase mask and the molded photopolymer, respectively. (e) SEM images of a top view of the surface embossed photopolymer. (f) High resolution SEM images of cross-sectional (top frame) and top views (bottom frame) of the molded photopolymer.

^{a)}Electronic mail: jrogers@uiuc.edu.

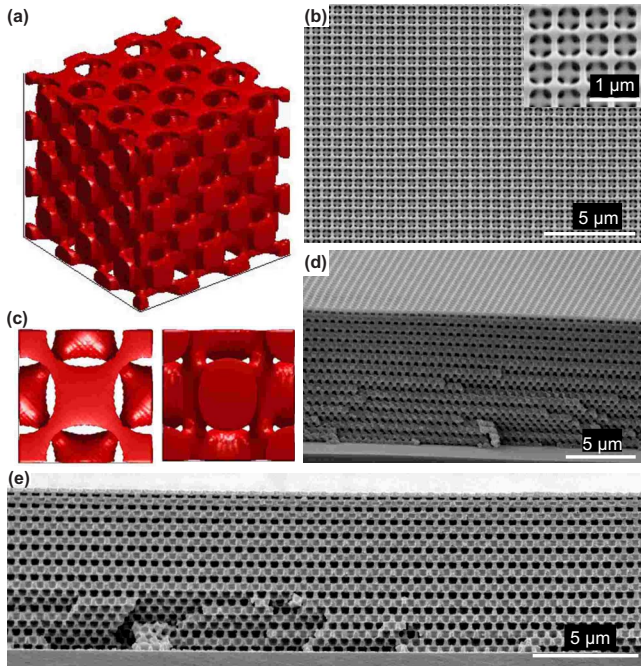


FIG. 2. (Color online) Optical simulations of the exposure process and resulting 3D polymer structures. [(a) and (c)] Angled view of multiple unit cells and top [(c), left frame] and side [(c), right frame] of computed 3D intensity distributions viewed after application of a binary cutoff filter to simulate the exposure and development process. [(b), (d), and (e)] SEM images of representative 3D structures formed in a photopolymer. (b) Large area top view, with high resolution inset. [(d) and (e)] Angled and cross-sectional views, respectively.

served as the light source. The pulse duration and coherence length of the laser and slight absorption in the SU8 limit the ultimate thicknesses of structures that can be formed in this fashion. For the experimental conditions examined, these limits correspond to a depth of $\sim 20 \mu\text{m}$, considerably larger than the thicknesses of structures investigated here. Laser output through a lens ($f=400 \text{ mm}$) with small convergence angle ($<10 \text{ mrad}$) provided peak powers sufficiently high to initiate 2ph absorption in SU8. For results presented here, the beam size ($\sim 3 \text{ mm}$ diameter) defined the exposure area. The use of circularly polarized light eliminated any polarization-induced spatial anisotropy.¹³ The molded relief produced five diffraction beams in SU8; their interference formed 3D intensity distributions that defined the exposure geometry. Distributions calculated using rigorous coupled wave analysis suggest a symmetry close to face-center cubic, with lattice parameters of 763 nm in plane and 789 nm out of the plane, as illustrated in Figs. 2(a) and 2(c). Images of representative 3D structures formed in this manner are presented in Fig. 2. Large area top view, angled view, and cross-sectional view are shown in Figs. 2(b), 2(d), and 2(e), respectively. Due to cross-linking reactions and other processes in the photopolymer, the 3D structures shrink, by 5%–10%, in the vertical dimension after developing. Lateral shrinkage was negligible due to adhesion to the substrate.

Structures with this geometry are of interest for photonic crystal applications, particularly when fabricated from materials that offer higher indices of refraction than the polymer used here. To explore this possibility, we formed silicon photonic crystals via a single step silicon inversion process with the 3D polymer structures as templates.⁷ SEM images of a representative Si structure are shown in Fig. 3 with a large

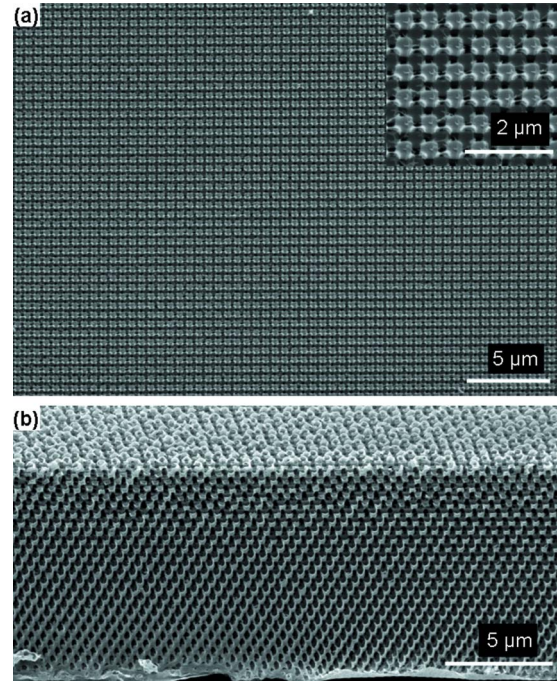


FIG. 3. (Color online) SEM images of a silicon structure formed using a corresponding polymer template. [(a) and (b)] Large area top and angled cross-sectional views of a typical sample, respectively. The inset in (a) shows a high resolution top view.

area and high resolution (inset) top view [Fig. 3(a)] and an angled cross-sectional view [Fig. 3(b)].

To characterize the quality of the structures and their optical properties, we performed normal incidence transmission and reflection measurements using an optical microscope (Bruker Optics Inc., Hyperion 1000) coupled to a Fourier transform infrared spectrometer (Bruker Optics Inc., Vertex 70), with a silver mirror and air for reflectance and transmittance references, respectively. Experimental and calculated spectra for the polymer template and silicon-air photonic crystal are shown in Figs. 4(a) and 4(b), respectively. The measurement spot size was $45 \mu\text{m}$, obtained with a $10\times$ objective lens and 0.45 mm spatial aperture. Due to the Gaussian intensity profile of the exposure laser beam, the sample experienced different exposure doses at different locations, leading to different shrinkage and fill fractions. These differences lead to variations in the strength of reflection peak and location of the center wavelength, as shown in the insets in Figs. 4(a) and 4(b). Due to this effect, and possibly other sources of slight nonuniformity, increasing the spot size to $110 \mu\text{m}$ led to reductions in reflectance by $\sim 10\%$. Despite this, the polymer structure exhibited a strong reflection peak ($\sim 65\%$) comparable to the best results obtained with the most advanced forms of interference lithography,⁸ and much better than previous reports ($\sim 30\%$).^{7,15–18} The silicon photonic crystal shows a broad reflection peak at slightly longer wavelengths and with higher reflectance ($\sim 80\%$), consistent with the comparatively higher index of refraction of the silicon. The peak reflection is significantly higher than the best previous reports (30%–50%) of silicon 3D photonic crystals formed by interference lithography.^{7,16}

In addition to the main reflection peak, other features in the spectra provide additional information on the properties of both the polymer and silicon photonic crystals. For ex-

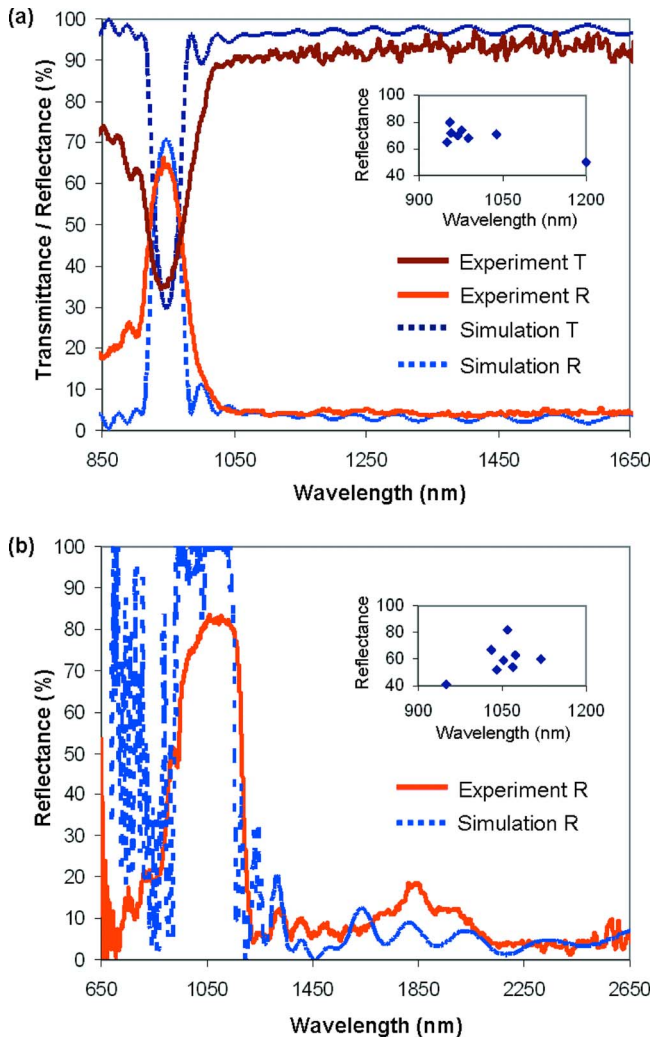


FIG. 4. (Color online) Measured and simulated normal incidence reflectance/transmittance spectra. [(a) and (b)] Results from a polymer structure and its silicon inverse structure, respectively. The dotted and solid lines in both frames correspond to simulation and experiment, respectively. The insets show the distribution of the center wavelength and peak reflectance determined by measurements of different locations of a representative structure.

ample, Fabry-Pérot (FP) fringes produced by reflections from the top and bottom surfaces are consistent with high structural quality.⁸ Together, FP fringes and SEM measurements provided information on filling fraction (i.e., fractional volume of polymer or silicon, to air) and structure periodicity. For the case of Fig. 4, the fill fraction for the polymer structure was 56.7% and the periodicity was 700 nm in the vertical direction ($\sim 10\%$ shrinkage). Simulations of silicon growth based on the parameters of polymer template suggested a pinch-off fill fraction of 14.5% for the silicon structure, in good agreement with that obtained experimentally [14%, estimated from the FP fringes in Fig. 4(b)]. Simulated reflection spectra were obtained using a one dimensional transfer matrix method⁸ and the finite-difference time-domain (FDTD) method with MIT electromagnetic equation propagation freeware for the polymer template and silicon structure, respectively. Compared to simulations, we observed slightly lower and broader reflection peaks in both polymer and silicon structures. The deviations can be attrib-

uted to slight sample inhomogeneities, light scattering due to surface roughness, and distortion associated with the fabrication processes. Since the FDTD simulations model silicon as a perfect dielectric material, discrepancies could be due to residual light absorption and scattering.

In conclusion, the results presented here demonstrate a very simple method to fabricate 3D structures that show photonic properties that are as good as or better than those obtained using other approaches. The scalability of the technique to large areas, its high throughput operation and experimental simplicity, combined with engineering flexibility in the geometries of the structures that are produced suggest a promising route to fabrication of photonic and other classes of 3D systems.

We acknowledge T. Banks and K. Colravy for help with processing using facilities at the Materials Research Laboratory. This work was supported by the DOE through Grant No. DE-FG02-07ER46471 and Sandia National Laboratories, a multiprogram laboratory operated by Sandia Corporation, a Lockheed Martin Company. This work was supported by the Division of Materials Science, Office of Basic Energy Science, for the U.S. Department of Energy's National Nuclear Security Administration under Contract No. DE-AC04-94AL85000. The facilities included the Materials Research Laboratory, University of Illinois, which is partially supported by the U.S. Department of Energy under Grants Nos. DE-FG02-07ER46453 and DE-FG02-07ER46471.

¹E. Yablonovitch, *Phys. Rev. Lett.* **58**, 2059 (1987).

²R. D. Meade, D. A. Devenyi, J. D. Joannopoulos, O. L. Alerhand, D. A. Smith, and K. Kash, *J. Appl. Phys.* **75**, 4753 (1994).

³A. Blanco, E. Chomski, S. Grabtchak, M. Ibisate, S. John, S. W. Leonard, C. Lopez, F. Meseguer, H. Miguez, J. P. Mondia, G. A. Ozin, O. Toader, and H. M. van Driel, *Nature (London)* **405**, 437 (2000).

⁴B. H. Cumpston, S. P. Ananthavel, S. R. Marder, and J. W. Perry, *Nature (London)* **398**, 51 (1999).

⁵G. M. Gratson, M. Xu, and J. A. Lewis, *Nature (London)* **428**, 386 (2004).

⁶M. Campbell, D. N. Sharp, M. T. Harrison, R. G. Denning, and A. J. Turberfield, *Nature (London)* **404**, 53 (2000).

⁷V. Ramanan, E. Nelson, A. Brzezinski, P. V. Braun, and P. Wiltzius, *Appl. Phys. Lett.* **92**, 173304 (2008).

⁸Y. C. Chen, J. B. Geddes III, J. T. Lee P. V. Braun, and P. Wiltzius, *Appl. Phys. Lett.* **91**, 241103 (2007).

⁹S. Jeon, J.-U. Park, R. Cirelli, S. Yang, C. E. Heitzman, P. V. Braun, P. J. A. Kenis, and J. A. Rogers, *Proc. Natl. Acad. Sci. U.S.A.* **101**, 12428 (2004).

¹⁰D. Shir, S. Jeon, H. Liao, M. Highland, D. G. Cahill, M. F. Su, I. F. El-Kady, C. G. Christodoulou, G. R. Bogart, A. V. Hamza, and J. A. Rogers, *J. Phys. Chem. B* **111**, 12945 (2007).

¹¹I. Bitá, T. Choi, M. E. Walsh, H. L. Smith, and E. L. Thomas, *Adv. Mater. (Weinheim, Ger.)* **19**, 3809 (2007).

¹²D. Chanda, L. Abolghasemi, and P. R. Herman, *Opt. Express* **14**, 8568 (2006).

¹³S. Jeon, V. Malyarchuk, J. A. Rogers, and G. P. Wiederrecht, *Opt. Express* **14**, 2300 (2006).

¹⁴S. Jeon, D. Shir, Y. S. Nam, and J. A. Rogers, *Opt. Express* **15**, 6358 (2007).

¹⁵J. S. King, E. Graugnard, O. M. Roche, D. N. Sharp, J. Scringeout, R. G. Denning, A. J. Turberfield, and C. J. Summers, *Adv. Mater. (Weinheim, Ger.)* **18**, 1561 (2006).

¹⁶J. H. Moon, S. Yang, W. Dong, J. W. Perry, A. Adibi, and S.-M. Yang, *Opt. Express* **14**, 6297 (2006).

¹⁷Y. C. Zhong, S. A. Zhu, H. M. Su, H. Z. Wang, J. M. Chen, Z. H. Zeng, and Y. L. Chen, *Appl. Phys. Lett.* **87**, 061103 (2005).

¹⁸J. Q. Chen, J. Q. Jiang, X. N. Chen, L. Wang, S. S. Zhang, and R. T. Chen, *Appl. Phys. Lett.* **90**, 093102 (2007).